Mean-time-to-failure study of flip chip solder joints on Cu/Ni(V)/Al thin-film under-bump-metallization

W. J. Choi,[a] E. C. C. Yeh,[b] and K. N. Tu[c]
Department of Materials Science and Engineering, UCLA, Los Angeles, California 90095-1595

(Received 27 May 2003; accepted 13 August 2003)

Electromigration of eutectic SnPb flip chip solder joints and their mean-time-to-failure (MTTF) have been studied in the temperature range of 100 to 140 °C with current densities of 1.9 to 2.75 $\times 10^4$ A/cm^2. In these joints, the under-bump-metallization (UBM) on the chip side is a multilayer thin film of Al/Ni(V)/Cu, and the metallic bond-pad on the substrate side is a very thick, electroless Ni layer covered with 30 nm of Au. When stressed at the higher current densities, the MTTF was found to decrease much faster than what is expected from the published Black's equation. The failure occurred by interfacial void propagation at the cathode side, and it is due to current crowding near the contact interface between the solder bump and the thin-film UBM. The current crowding is confirmed by a simulation of current distribution in the solder joint. Besides the interfacial void formation, the intermetallic compounds formed on the UBM as well as the Ni(V) film in the UBM have been found to dissolve completely into the solder bump during electromigration. Therefore, the electromigation failure is a combination of the interfacial void formation and the loss of UBM. Similar findings in eutectic SnAgCu flip chip solder joints have also been obtained and compared. © *2003 American Institute of Physics.* [DOI: 10.1063/1.1616993]

I. INTRODUCTION

In mainframe computers, area array of solder bumps has been used to connect Si chips to first level packaging substrates.[1] The trend of miniaturization continues to scale down the bump pitch and diameter,[2] increasing current density in the solder bumps. At present, each solder bump is designed to carry 0.2 A, but it will soon be 0.4 A. For a bump of 100 μm or less in diameter, the average current density will be higher than 1×10^4 A/cm^2, and electromigration will become a reliability problem.[3–6] In this article, we show that the unique configuration of a flip chip (FC) solder joint has led to serious current crowding. It is the much higher current density in the current crowding region that has caused the solder joint to fail by interfacial void formation at the cathode end. We have also examined the phase change in the thin-film under-bump-metallization (UBM) during current stressing, and we found that the films dissolved and disappeared completely into the solder bump.

A solder joint consists of three parts: solder bump, thin-film UBM on the chip side, and metallic bond-pad on the substrate side.[1] The UBM is the contact between the solder bump and the on-chip Al interconnect lines. The bond-pad is the contact between the solder bump and the Cu trace on the substrate. We have used simulation to show that the unique line-to-bump configuration has produced a very large current crowding near their contact, especially at the contact between the solder bump and the on-chip UBM. The simulated current crowding distribution matches the location of electromigration-induced void formation or electrical open failure in the solder bump.[7]

Furthermore, we found that the mean-time-to-failure (MTTF) of solder joints is greatly affected by the current crowding. We measured the MTTF with different current densities and temperatures in both eutectic SnPb and eutectic SnAgCu FC solder joints. The higher the applied current density, the greater the current crowding and, in turn, the shorter the MTTF. Indeed, the MTTF has been found to be much shorter than the predicted value based on Black's equation.

II. EXPERIMENTAL PROCEDURE

A schematic diagram of the cross-section of FC solder joint samples used for electromigration test is shown in Fig. 1. Two eutectic SnPb solder bumps were electrically connected by a thin Al interconnect line on the Si chip. The UBM on the chip side was a sputtered multilayered thin film of Cu/Ni(V)/Al, each layer of which is about 300 to 400 nm in thickness. In the Ni(V) layer, the concentration of V is about 7 at. %. The purpose of adding V to Ni is to enhance the sputtering rate of Ni by reducing the magnetic interference of Ni. The bond-pad on the FR4 substrate side was a bilayer film of Au/Ni on Cu trace, where the Au is 30 nm and the Ni is very thick—over 10 μm. The solder bump joins the Cu film on the chip side to the Au film on the substrate side. The gap between the chip and FR4 substrate was underfilled with epoxy. During electromigration tests, the samples were kept on a hot plate at temperatures of 100, 125, and 140 °C with current densities of 1.90, 2.25, and 2.75×10^4 A/cm^2. Electrical potential was checked every minute during the test, and MTTF was determined by an abrupt potential increase in the potential–time curve.

[a]Now at: Intel, Chandler, AZ.
[b]Now at: Intel, Santa Clara, CA.
[c]Electronic mail: kntu@ucla.edu

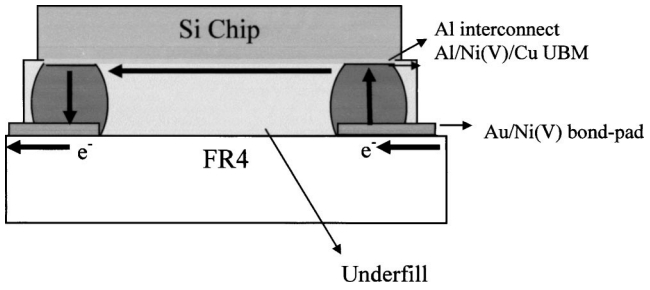

FIG. 1. Schematic diagram of FC solder joint sample for electromigration tests.

To investigate the microstrucutural change and the failure mode in a solder joint induced by the electromigration tests, a set of solder bumps was cross-sectioned after current stressing at various periods of time and examined by scanning electron microscopy (SEM). Certain solder joints were cross-sectioned before electromigration test so that the microstructural change on the cross-sectioned surface can be observed *in situ* during electromigration. Figure 2 shows the cross sections of a set of four solder joints, where each of them was tested for a different period of time. The examination of microstructure and morphological changes in the solder bump as well as the intermetallic compound (IMC) formed between the solder and the UBM will be explained later.

The current density distribution in a solder joint has been simulated by a two-dimensional model. The simulation indicates a very serious current crowding distribution in the line-to-bump configuration of a FC solder joint, to be presented.

The MTTF of eutectic SnAgCu solder joints was also investigated by the same method as the eutectic SnPb. The UBM and bond-pad are the same as those used in the eutectic SnPb. However, the test temperatures were 125, 140, and 160 °C, and the test current densities were 2.25×10^4, 2.75×10^4, and 3.0×10^4 A/cm^2. These test conditions were more severe than those used for the eutectic SnPb. It is because of the higher melting temperature of the Pb-free solder and the longer MTTF observed.

III. RESULTS

A. MTTF measurement

The measured MTTF of eutectic SnPb solder bumps is shown in Table I. The value listed in the table is the averaged value of three samples tested. We recall that similar experiments were performed with the same kind of samples at

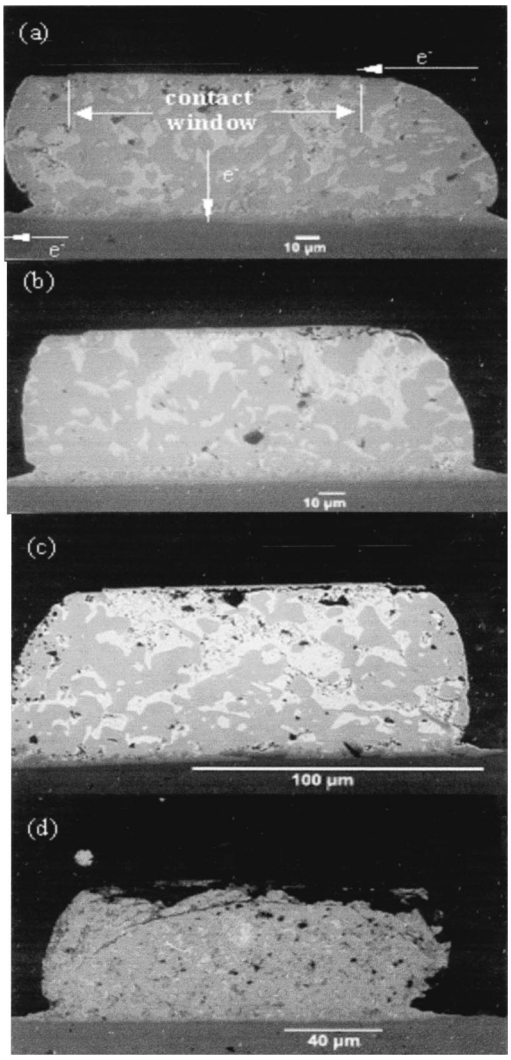

FIG. 2. SEM images of a sequence of void propagation in the cathode end of eutectic SnPb FC solder joints at 125 °C and 2.25×10^4 A/cm^2: (a) 37, (b) 38, (c) 40, and (d) 43 h.

lower current densities by Brandenburg and Yeh.[3] They showed that the MTTF obeys Black's equation[8]

$$\mathrm{MTTF}=A\frac{1}{j^n}\exp\left(\frac{Q}{kT}\right), \tag{1}$$

where A is constant, j is current density, n is a model parameter for current density, Q is activation energy, k is Boltzmann's constant, and T is average bump temperature. They found that $n=1.8$ and $Q=0.8$ eV. This n value is quite reasonable as compared to $n=2$ in the model proposed by

TABLE I. MTTF of eutectic SnPb FC solder joints.

	1.5 A (1.9×10^4 A/cm^2)		1.8 A (2.25×10^4 A/cm^2)		2.2 A (2.75×10^4 A/cm^2)	
	Calculated (h)	Measured (h)	Calculated (h)	Measured (h)	Calculated (h)	Measured (h)
100 °C	···	···	380	97	265	63
125 °C	108	573[a]	79.6	43	55.5	3
140 °C	46	121	34	32	24	1

[a]Not failed.

TABLE II. Measured MTTF of eutectic SnAgCu FC solder joint.

	1.8 A (2.25×10^4 A/cm^2)	2.2 A (2.75×10^4 A/cm^2)	2.4 A (3.0×10^4 A/cm^2)
125 °C	580 h	112 h	83 h
140 °C	132 h	94.5 h	14.2 h
160 °C	99 h	21 h	2 h

Black, and the measured activation energy is a little bit larger than the activation energy of lattice diffusion in eutectic SnPb solder.

If we take $n=1.8$ and $Q=0.8$ eV and apply them to our experimental conditions, the expected MTTF values were calculated on the basis of Eq. (1) and given in Table I. However, in comparison to our measured values as shown in Table I, our measured MTTF at 1.9×10^4 A/cm^2 is slightly longer than the expected, and yet the measured is much shorter than the expected at the higher current densities of 2.25×10^4 and 2.75×10^4 A/cm^2. Especially at the most severe condition of 2.75×10^4 A/cm^2 and 140 °C, the measured MTTF was only 1 h, but the expected is 24 h.

The results of MTTF measurement for the Pb-free solder bump (eutectic SnAgCu) are shown in Table II. When we compare the MTTF of eutectic SnPb with that of eutectic SnAgCu, the latter is found to be much longer than the former. For example, at the same test condition of 125 °C and 2.25×10^4 A/cm^2, the eutectic SnPb solder bump failed after 43 h, but the eutectic SnAgCu solder failed after 580 h. The eutectic SnAgCu solder bump lasts more than 10 times longer than the eutectic SnPb.

B. Void propagation and current crowding

Figure 2 shows a sequence of interfacial void propagation and the catastrophic failure in the eutectic SnPb solder bump. The tested condition was 2.25×10^4 A/cm^2 at 125 °C. Figure 2(a) shows the solder bump after 37 h of electromigration or current stressing. Until this time no void was found. The black spots in the solder bump are not voids, but they are polishing debris. It is possible that some of the black spots are voids in the solder bump left behind by the reflow of the solder paste. After 38 h of current stressing, voids were observed at the cathode, the top corner on the right-hand side of the solder bump [see Fig. 2(b)], and these voids propagated along the interface with further stressing [see Fig. 2(c)]. After 43 h of stressing, the solder bump is completely failed, [see Fig. 2(d)]. This failure sequence is the same in the eutectic SnAgCu solder bumps and is shown in Fig. 3.[9]

Figure 4(a) shows the potential versus time curve of a sample tested at 2.25×10^4 A/cm^2 and 125 °C. This curve corresponds to those solder bumps shown in Fig. 2. Before the complete failure, as shown in Fig. 2(d), the potential or resistance of the sample did not change much, even though void propagation had covered a large area of the contact window, as shown in Figs. 2(b) and 2(c). This is due to the small dimension of the Al line as compared to that of the solder joint, so that almost all the resistance is taken up by the line. As the void propagates from right to left, the entrance of the current into the solder bump will be displaced to the front of the void, as shown in Fig. 4(b). It moves with the front of the void. As long as the current can enter the solder joint, the void has very little effect on the resistance change as a whole. The potential curve remains flat, as shown in Fig. 4(a). Only when the void extends across the entire contact area, the potential or resistance will show an abrupt jump, indicating the failure of the solder joint. The behavior shows that in order to detect the early stage of failure of a flip chip solder joint, the Wheatstone bridge method of resistance change measurement is more sensitive than the four-point-probe method.[10]

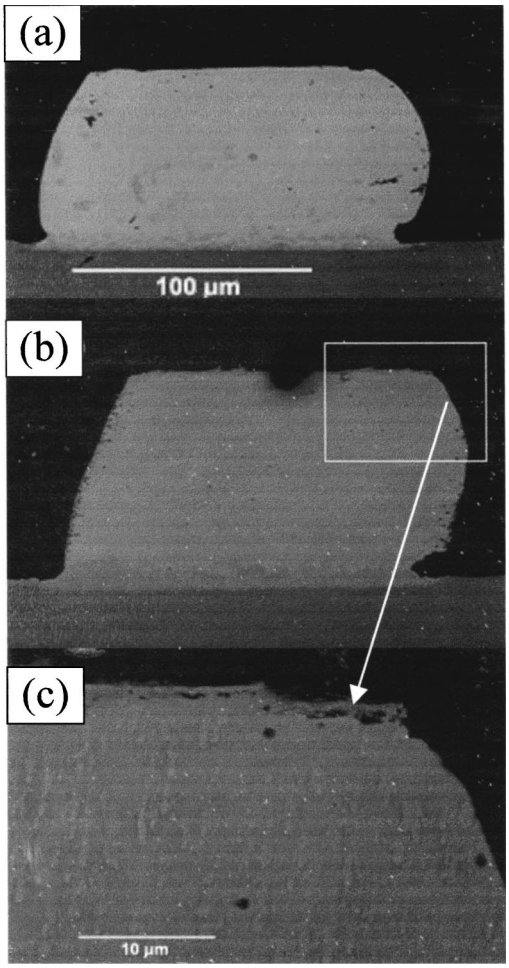

FIG. 3. SEM images of a sequence of void propagation in the cathode end of eutectic SnAgCu FC solder joints at 140 °C and 3.0×10^4 A/cm^2: (a) 0, (b) 14, and (c) magnified image of (b).

C. Dissolution of intermetallic compound and Ni UBM

To observe the *in situ* change of the solder bump in electromigration, the sample was cross-sectioned before the current stressing. Figure 5(a) is the SEM image of the cross-sectioned solder ball after current stressing at 2.25×10^4 A/cm^2 at 125 °C for 113 h. The mass migration is observed in the form of domain popping up in the anode side. In Figs. 5(b) and 5(c), the cathode side of the solder

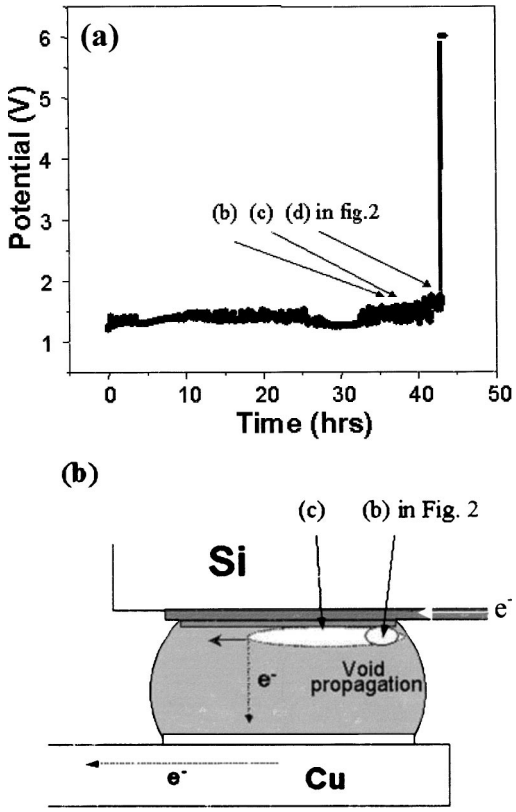

FIG. 4. (a) Time vs potential curve during current stressing of a eutectic SnPb solder joint and (b) schematic diagram of void propagation along the cathode interface.

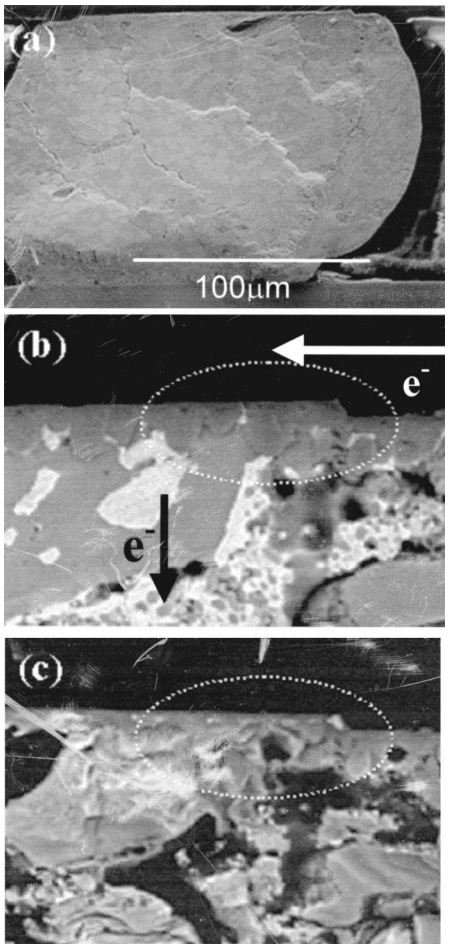

FIG. 5. (a) SEM image of a cross-sectioned solder bump after current stressing of 113 h at 125 °C and 2.25×10^4 A/cm^2. A very rough surface morphology induced by electromigration can be seen. Magnified SEM images of the right top corner of the eutectic SnPb solder joint (b) before and (c) after 113 h of current stressing at 125 °C and 2.25×10^4 A/cm^2.

bump is magnified before and after the stressing, respectively. They showed the dissolution of IMC in the circle in Fig. 5(c) as compared to that in Fig. 5(b).[11]

Figure 6 shows the effect of electromigration on the Ni(V) UBM. The test condition was the same as that in Fig. 2. The Ni concentration measured by x-ray absorption mapping in a pair of solder joints and the corresponding SEM images are shown in Fig. 6. Figs. 6(a) and 6(c) show, respectively the SEM image and x-ray mapping of Ni of the solder bump that has experienced the electron flow from the substrate side (bottom) to the chip side (top). Figures 6(b) and 6(d) show, respectively, the SEM and x-ray mapping of the sample that has experienced the opposite direction of electron flow. In Fig. 6(c), a concentration of Ni at the top interface is revealed. But in Fig. 6(b), no such Ni concentration was found after the complete failure, indicating that all the Ni UBM was dissolved during the current stressing. The concentration of the element V in Ni(V) is too small to be detected.

D. Joule heating

Due to the high resistance of Al line and current crowding, the real temperature in the solder bump must be higher than the test temperature in the ambient because of Joule heating. We attempted to measure the real temperature of the solder joint by applying a coating of a crayon on the cross-sectioned surface of a solder joint. A set of crayons was used that has a ladder sequence of melting temperatures. The cross-sectioned solder was stressed at an ambient temperature of 125 °C. When the crayon melts, the sample temperature is higher than the melting temperature of this specific crayon. However, the next crayon, which has a melting point a ladder step above the specific one, did not melt. We can determine the sample temperature to be between them: one above it and one below it. The results are given in Table III.

IV. DISCUSSION

In Table I, the measured MTTF is much shorter than the expected at the higher current density. There are three reasons the failure is faster: (1) current crowding, (2) dissolution of intermetallic compound and Ni UBM, and (3) Joule heating.

A. Current crowding

The Black's equation of MTTF was derived from electromigration experiments of straight Al lines. The geometry of a straight Al line is very different from that of a FC solder joint. In Fig. 7, it is depicted that the diameter of a solder bump is about two orders of magnitude larger than the thickness of an Al line: 100 versus 1 μm. Assuming the width of

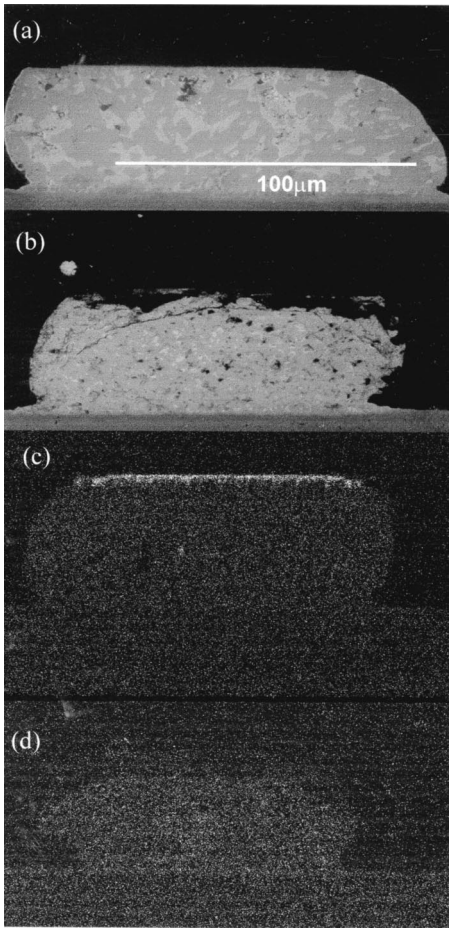

FIG. 6. SEM and energy dispersive x-ray (EDX) mapping of FC solder joints with a diameter of 125 μm. (a) SEM image of an unfailed sample, in which the electrons flowed from the substrate to the chip; (b) SEM image of a failed sample, in which the electrons flowed from the chip to the substrate; (c) EDX mapping of Ni for the unfailed sample; and (d) EDX mapping of Ni for the failed sample.

the Al line is the same as the diameter of the solder bump, the average current density in the Al line is two orders of magnitude higher than that in the solder bump when the same current is conducted between them. Hence, the current density changes dramatically between them. In other words, there must be a current crowding near the contact area between them.

A two-dimensional simulation of current distribution in a FC solder joint is shown in Fig. 8. In this simulation, the design rule that each bump carries 0.2 A was applied. We assumed that the thickness of the metal line connecting the

TABLE III. Real device temperature of eutectic SnPb flip chip solder joints measured by crayon melting.

Melting temp. of crayon (°C)	Crayon melting or not	Comparison with ambient temp. of 125 °C
121	Melting	4 °C lower
135	Melting	10 °C higher
149	Melting	24 °C higher
163	Melting	38 °C higher
177	Not melting	52 °C higher

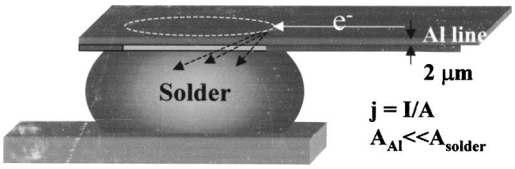

FIG. 7. Schematic diagram depicting a very large current density change at the contact interface between a solder joint and the interconnect above it.

solder bump was 2 μm, and the contact window between them was 100×100 μm^2. In Fig. 8(a), the highest current density of 3×10^4 A/cm^2 due to current crowding occurs inside the contact window at the top on the right hand side of the solder bump. This current density is more than ten times higher than the averaged current density of 2×10^3 A/cm^2 inside the solder bump. The current distribution in the cross section of the solder joint is shown in Fig. 8(b). According to previous reports,[12–15] vacancies move from high to low current density region because of the current density gradient force in current crowding. This has been observed near the current crowding region in the solder bump. We examine the top corner region in the right-hand side in Figs. 2(b) and 3(c), that is, the region just below the passivation layer (outside the contact window), there should be no current density. On the other hand, in the neighboring region inside the contact window, the current density is the highest due to current crowding because it is the entrance where the current enters the bump. However, voids are observed below the passivation layer, where there is no current. Therefore, the vacancies are driven by the gradient force to move from the highest current density region in the contact window to the no current density region below the passivation layer. When the vacancies reach supersaturation, voids nucleate there and

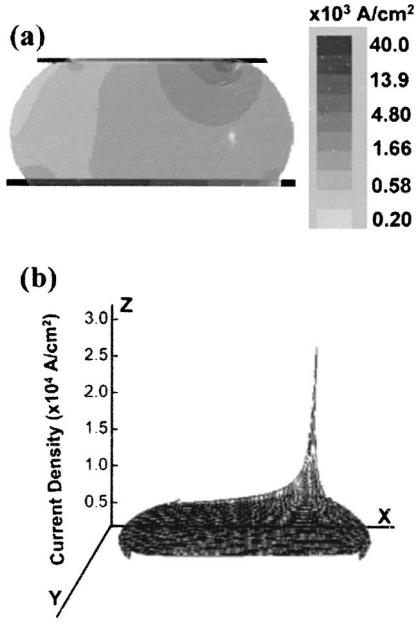

FIG. 8. A two-dimensional simulation of current distribution in the solder joint. (a) Current distribution in the cross-section of a solder joint. (b) The cross-section is plotted on the $X-Y$ plane and the current density is plotted along the Z-axis. The current enters the solder bump from the upper-right corner where current crowding occurs.

propagate along the interface between the UBM and solder bump. Eventually, it leads to an open failure. When such a failure mode was monitored by resistance change, a typical curve of resistance change vs. time has been shown in Fig. 4(a). It is insensitive to the interfacial void growth because the solder bump has low resistance. In other words, a partial area change of the contact interface does not affect the total resistance change.

To have the complete failure, it took 43 h at 125 °C and 2.25×10^4 A/cm^2. When tested at this condition up to 37 h, no void was found. After 38 h, void initiated and propagated, it then caused a complete failure very quickly. From void initiation to failure, it took only 5 h. Compared to the total time of failure of 43 h, it is only 10%, so the other 90% is incubation time. This means that the nucleation of the void dominates the MTTF of the solder bump.

B. Dissolution of intermetallic compound and Ni UBM

The role of intermetallic compound in a solder joint is to serve as the interphase (diffusion barrier) between the solder and the UBM and to preserve the joining of the solder joint. If the IMC is removed, the joint is no longer reliable.

In Fig. 5(b), the scallop shaped Cu-Sn IMC adheres very well to the UBM before current stressing. But in Fig. 5(c) after current stressing, the IMC dissolved or disappeared into the solder bump. After that, the underlying Ni(V) layer is exposed to the solder. It enables the solder to react with the Ni UBM. The solder and Ni may react to form Ni-Sn IMC, yet it will be dissolved as the Cu-Sn IMC. When all the Ni(V) is dissolved into the solder, the next metal layer to be exposed is Al. Since the solder will not adhere to Al, the joint is weakened. This can also allow the void to nucleate and propagate more easily along the weakened interface between solder and Al. Hence, it is likely that part of the incubation time may be spent to dissolve the UBM. The dissolution is enhanced under current crowding in the entrance to the solder bump.

C. Joule heating

Another reason for faster MTTF may be due to Joule heating. The Joule heating of the Al line can be transferred to the contact between the line and the solder bump, and the current crowding can generate more heat around the contact. The measured temperature increase is about 40 °C as shown in Table III for the eutectic SnPb solder joints. It is substantial and can affect MTTF greatly. For example, if the annealing temperature is 140 °C, the real sample temperature due to Joule heating can be about 180 °C. It is very close to the melting temperature of eutectic SnPb solder at 183 °C, therefore, atomic diffusion is much enhanced, which will shorten the MTTF. We note that since the current density and microstructure of eutectic SnPb are different from those of eutectic SnAgCu, the temperature increase due to Joule heating in the latter could be different.

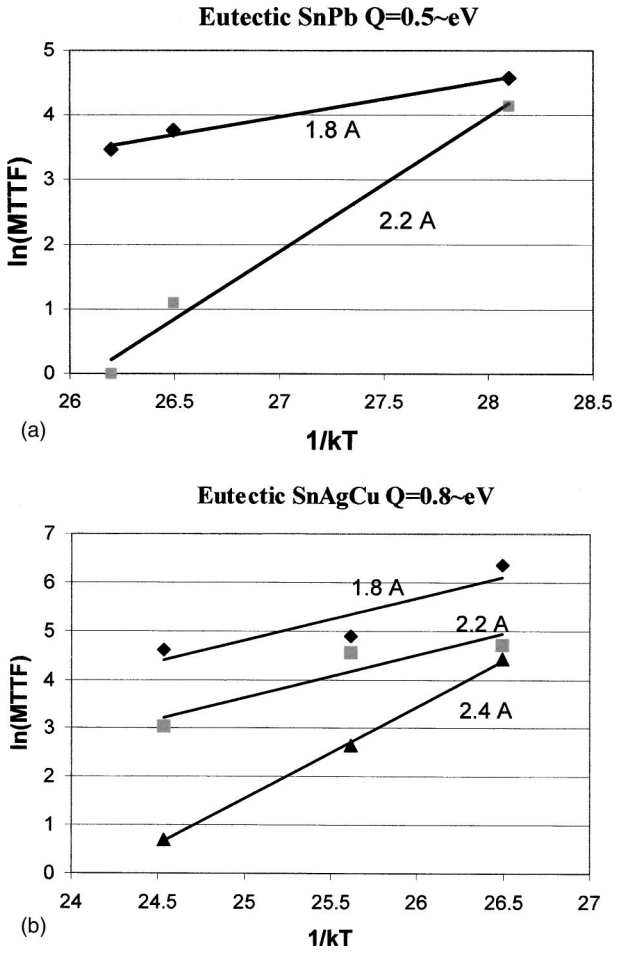

FIG. 9. Plots of MTTF against $1/k(T+\Delta T)$, where ΔT is the temperature increase due to Joule heating: (a) eutectic Sn Pb solder joints, and (b) eutectic SnAgCu solder joints.

D. Analysis of Black's equation for MTTF of FC solder joints

Because of the discrepancy between the measured MTTF and the calculated MTTF based on Eq. (1), we now examine and analyze the parameters in Eq. (1). There are four of them; j, n, Q, and T. On the basis of our simulation, the effect of current crowding is to increase the average current density j by almost a factor of 10. Due to Joule heating, the solder joint temperature has been increased by about 40 °C. To include these effects in MTTF analysis, we have attempted to modify Black's equation by multiplying j with a factor c and adding to T an increment of ΔT:

$$\mathrm{MTTF}=A\frac{1}{(cj)^n}\exp\left[\frac{Q}{k(T+\Delta T)}\right]. \tag{2}$$

In Eq. (2), if we keep both n and Q constant, we see that the effect of both c and ΔT is to reduce MTTF. Both of them should depend on the applied current density. However, we have taken $c=10$ and $\Delta T=40$ °C in the present analysis for both the solder joints. A constant c can be combined with the constant A, so that it has no effect on Q. When the measured MTTF is plotted against temperature $(T+\Delta T)$ as shown in Figs. 9(a) and 9(b), the calculated activation energy Q is

found to be 0.5 and 0.8 eV for the eutectic SnPb solder and eutectic SnAgCu solder, respectively.

When we calculated the activation energy, the data from the highest current density of the eutectic SnPb solder joint were excluded in Fig. 9(a) because the modified temperature is too close to the melting point of the solder. We note that the temperature increase of 40 °C was measured on the cross-sectioned solder bump. When we cross-sectioned the solder bump, about 20% of the Al interconnection line was polished away. Therefore, the total current in the Al line in the cross-sectioned sample is smaller than the unsectioned sample. Hence, the Joule heating could be larger in the unsectioned sample, so the temperature increase could be higher than we measured. This larger Joule heating could cause local melting of the solder bump, especially at the current crowding region. Therefore, only two data points from the relatively lower current density tests were used to calculate the activation energy of the eutectic SnPb solder joint. Since the device operation temperature is about 100 °C, there is little room for accelerated tests of eutectic SnPb solder joints.

The physical meaning of Q in Eq. (1) has been taken to be the activation energy of lattice diffusion in the solder joint. Near the melting temperature, if we assume the lattice diffusivity D to be 10^{-8} cm^2/s and the diffusion time t to be 1 h, which is the shortest MTTF measured, we have a diffusion distance of $x=120\ \mu$m when we take $x^2=4Dt$.[16] It is as large as the diameter of a solder joint. This means that the lattice diffusion is fast enough. Even at the lower annealing temperature of 100 °C, the lattice diffusion is fast because the Joule heating has increased the temperature to 140 °C.[17] Therefore, the vacancies needed in nucleation and growth of a void at the cathode end can be supplied by the lattice diffusion from the anode end. On the other hand, the growth of an interfacial void, as depicted in Fig. 4(b), can also occur by interfacial diffusion. In other words, vacancies can be supplied by interfacial diffusion from the surface of the bump near the cathode rather than by lattice diffusion all the way from the anode. The activation energy of interfacial diffusion will be much less than that of lattice diffusion.

We recall that, as shown in Fig. 5, the MTTF for a sample stressed at 125 °C with a current density of 2.25×10^4 A/cm^2 was 43 h. However, 90% of the time was spent in void nucleation and only 10% of it was spent to propagate (or to grow) the void. In this case, the measured activation energy is more likely to be the sum of activation energy of nucleation and activation energy of diffusion. On the other hand, in the extreme case of stressing at the high current density of 2.75×10^4 A/cm^2 at 140 °C, the failure time was only 1 h. It is unclear in this case what the partition of time is between void nucleation and growth.

In view of the discrepancy and uncertainty discussed here, we can only conclude that we may not apply Black's equation to MTTF of FC solder joints without more studies. We should not attempt to interpret the activation energies shown in Fig. 9 until a better physical picture of failure is available.

V. CONCLUSION

Electromigration tests in flip chip eutectic SnPb solder joints were performed at 100, 125, and 140 °C, and at 1.90×10^4, 2.25×10^4, and 2.75×10^4 A/cm^2. The measured MTTF was found to be much smaller at the higher current density than the calculated values from the published Black's equation. The fast failure is due to current crowding, IMC dissolution, and Joule heating. By simulation of current distribution in a flip chip solder bump, we confirmed the existence of current crowding. In eutectic SnAgCu solder joints, the failure mode is the same as the eutectic SnPb. However, the Pb-free has a longer MTTF.

ACKNOWLEDGMENT

The authors would like to acknowledge the support by NSF Contract No. DMR-9987484 and SRC Contract No. NJ-774. The flip chip samples were provided by Dr. H. Balkan of Flip Chip Technologies.

[1] K. Puttlitz and P. A. Totta, *Area Array Technology Handbook for Microelectronic Packaging* (Kluwer Academic, Norwell, MA, 2001).
[2] C. S. Chang, A. Oscilowski, and R. C. Bracken, IEEE Circuits Devices Mag. **14**, 45 (1998).
[3] S. Brandenburg and S. Yeh, *Surface Mount International Conference and Exposition, SMI 98 Proceedings*, 1998, p. 337.
[4] C. Y. Liu, C. Chen, and K. N. Tu, J. Appl. Phys. **88**, 5703 (2000).
[5] T. Y. Lee, K. N. Tu, S. M. Kao, and D. R. Frear, J. Appl. Phys. **89**, 3189 (2001).
[6] W. J. Choi, E. C. C. Yeh, and K. N. Tu, *52nd ECTC Proceedings*, 2002, p. 1201.
[7] E. C. C. Yeh, W. J. Choi, K. N. Tu, P. Elenius, and H. Balkan, Appl. Phys. Lett. **80**, 580 (2002).
[8] J. R. Black, IEEE Trans. Electron Devices **ED-16**(4), 338 (1969).
[9] S.-Y. Jang, J. Wolf, W.-S. Kwon, K.-W. Paik, *52nd ECTC Proceedings*, 2002, p. 1206.
[10] M. Ding, H. Matsuhashui, P. S. Ho, A. Marathe, R. Master, and V. Pham, *Proceedings of the 2003 International Reliability Physics Symposium (IRPS)*, Dallas, TX, 30 March to 3 April, 2003.
[11] T. Y. Lee, K. N. Tu, and D. R. Frear, J. Appl. Phys. **90**, 4502 (2001).
[12] K. N. Tu, C. C. Yeh, C. Y. Liu, and C. Chen, Appl. Phys. Lett. **76**, 988 (2000).
[13] J. R. Lloyd, Appl. Phys. Lett. **79**, 1061 (2001).
[14] K. N. Tu, Appl. Phys. Lett. **79**, 1063 (2001).
[15] E. C. C. Yeh and K. N. Tu, J. Appl. Phys. **88**, 5680 (2000).
[16] P. G. Shewmon, *Diffusion in Solids* (McGraw-Hill, New York, 1963).
[17] D. Gupta, K. Vieregge, and W. Gust, Acta Mater. **47**, 5 (1999).